

AD-A077 450

NAVAL RESEARCH LAB WASHINGTON DC

F/G 9/5

THE INSTABILITY BOUNDARY AND GROWTH RATE CONTOURS OF THE GYROTR--ETC(U)

NOV 79 J Y CHOE , S AHN

UNCLASSIFIED

NRL-MR-4106

NL

1 OF 1

AD
A077450



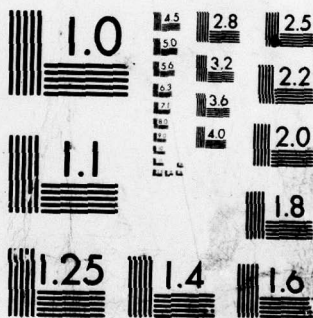
END

DATE

FILMED

1-80

DDC



MICROCOPY RESOLUTION TEST CHART
NATIONAL BUREAU OF STANDARDS-1963-A

12

NRL Memorandum Report 4106

LEVEL II

The Instability Boundary and Growth Rate Contours of the Gyrotron Amplifier with Spreads in Energy and Momenta

JOON Y. CHOE AND SAHYOUNG AHN

*Microwave Tube Staff
Electronics Technology Division*

DDC
RECEIVED
DEC 3 1979
E

November 14, 1979



NAVAL RESEARCH LABORATORY
Washington, D.C.

Approved for public release; distribution unlimited

79 11 30 057

AD A 077 450

DDC FILE COPY

THE INSTABILITY BOUNDARY AND GROWTH RATE CONTOURS OF THE GYROTRON AMPLIFIER WITH SPREADS IN ENERGY AND MOMENTA

The mechanism of the electron cyclotron maser instability¹⁻³ has been used successfully in the gyrotron oscillator⁴ which provides a powerful source of millimeter and submillimeter microwave generation. Many reviews on the developments of theories and experiments of the gyrotron already exist in the literature.⁵⁻⁶

Recently the bandwidth and linear growth rate of a gyrotron amplifier has been investigated in theories⁷⁻⁹ and experiments.^{10,11} The measured linear gain of a gyrotron amplifier lies in the predicted range of the growth rate. Its poor efficiency¹⁰ however was attributed to the velocity spread effect, i.e., the spreads in momentum and energy. It is our objective to investigate the effects of the spreads on the linear growth rates over a wide range of the mode spectra.

We consider a gyrotron amplifier which consists of the metallic cylindrical waveguide with radius R , and the annular tenuous electron beam under the uniform axial magnetic field B_0 inside the waveguide. We choose the equilibrium distribution function of beam electrons f_0 , given in terms of the total relativistic mass factor γ , the axial linear momentum p_z , and the azimuthal canonical angular momentum P_θ , to be a rectangular type function in γ , p_z and P_θ with the mean values given by $\hat{\gamma}$, \hat{p}_z and \hat{P}_θ , and their spreads by

Note: Manuscript submitted September 11, 1979.

$\hat{\gamma}\epsilon_\gamma$, $\hat{p}_z\epsilon_z$ and $\hat{p}_\theta\epsilon_\theta$ (Fig. 1). The linear dispersion relation for a $TE_{\ell ns}$ mode is then obtained for the eigenfrequency ω at the azimuthal mode number ℓ , the radial mode number n , and the magnetic harmonic number s , as a function of the axial wave number k .

In order to be manageable we assume that the spreads are not large such that only their effects on the resonance terms are kept,¹² and further assume that the growth rate is small, i.e., $|\omega_i| \ll \omega_c/\hat{\gamma}$, where $\omega_c \equiv |e| B_0/mc$. Then the dispersion equation is reduced to the equation*

$$\Delta + a + \eta b F(\Delta, \epsilon_\gamma, \epsilon_z) = 0, \quad (1)$$

where $\Delta \equiv \omega - \Omega_s$ represents the eigenfrequency shift from the Doppler-shifted cyclotron frequency of beam electrons Ω_s , defined by $\Omega_s \equiv kc\beta_z + s\omega_c/\hat{\gamma}$; $a \equiv (\Omega_s^2 - \omega_{\ell n}^2)/2\Omega_s$ refers to the degree of the synchronization between the beam mode Ω_s and the waveguide mode $\omega_{\ell n}$ defined by $\omega_{\ell n}^2 = c^2 k^2 + \omega_{co}^2$ with ω_{co} as the cutoff frequency; $b \equiv (\Omega_s^2 - c^2 k^2)/2\Omega_s$ measures the available energy; and η is the beam-waveguide coupling coefficient.¹³ Here $c\beta_z$ is the average axial velocity of electrons. The small growth rate assumption ($|\Delta| \ll \omega_c/\hat{\gamma}$) favors the instability term (proportional to Δ^{-2}) over the stabilizing terms (proportional to Δ^{-1} or Δ^0) in the dispersion equation. Consequently equation (1) slightly overestimates the actual growth rate. The information on the influence of the spreads are contained in function F , defined by

* Equation (1) was first obtained by Uhm and Davidson (i.e., see Eq. 29 of the paper; Phys. Fluids 22, September 1979) for the TE_{0n} mode. Here we generalized the case to the azimuthally asymmetric $TE_{\ell n}$ mode. The analysis is carried out in this report such as to keep the combined effect of both spreads maintained for the arbitrary axial wave number k .

$$F \equiv \frac{1}{4\epsilon_1\epsilon_2} \ln \left[\frac{\Delta^2 - (\epsilon_1 - \epsilon_2)^2}{\Delta^2 - (\epsilon_1 + \epsilon_2)^2} \right] \quad (2)$$

where $\epsilon_1 \equiv |\Omega_s| \epsilon_\gamma$ and $\epsilon_2 \equiv |kc\beta_z| \epsilon_z$. The function F is interchangeable with respect to ϵ_1 and ϵ_2 , and an even function of ϵ_1 and ϵ_2 ; $F(\Delta, \epsilon_\gamma = \epsilon_z = 0) = \Delta^{-2}$ recovers the dispersion relation without spread.¹³ Since the effects of ϵ_γ and ϵ_z are weighted by $|\Omega_s|$ and $|kc\beta_z|$, we find that the influence of the energy spread is dominant over that of the axial momentum for small $|k|$, while for large $|k|$ the reverse is true. In usual gyrotron devices, the wavenumber k is commonly chosen such that ϵ_1 and ϵ_2 are in the same order of magnitude.

The growth rate, viz. the imaginary part of Δ , depends on several experimental parameters: V (beam voltage), I (beam current), β_1/β_z (ratio of the velocity in perpendicular to axial direction), r_0 (beam center location), s , ℓ , n , R and k in addition to ϵ_γ and ϵ_z . By introducing a normalization equation

$$Q \equiv (\eta b)^{1/3} \tilde{Q}, \quad (3)$$

the dispersion equation (1) becomes

$$\tilde{\Delta} + \tilde{a} + F(\tilde{\Delta}, \tilde{\epsilon}_1, \tilde{\epsilon}_2) = 0 \quad (4)$$

The advantage of normalization (3) becomes apparent when we note that the reduced dispersion equation (4) now becomes a function of mere dimensionless numbers $\tilde{\Delta}$, \tilde{a} , $\tilde{\epsilon}_1$ and $\tilde{\epsilon}_2$ and that the experimental parameters are absorbed in normalizing factor $(\eta b)^{1/3}$. The scaling factor $(\eta b)^{1/3}$, \tilde{a} , $\tilde{\epsilon}_1/\epsilon_\gamma$, and

$\tilde{\epsilon}_2/\epsilon_z$ as functions of the wave number k are illustrated in Fig. 2. It shows a TE_{011} mode with $V = 71.5$ kV, $I = 9.5$ A, $\beta_{\perp}/\beta_z = 1.5$, and r_0 and R optimized to give highest growth rates.¹⁰ Note that $\tilde{a} \geq 0$ for $\Omega_s \geq \omega_{ln}$ and the upper limit of \tilde{a} is determined by the wall radius R . We also note that the scaling factor $(\eta b)^{1/3}$ is in the order of 10^{-2} and remains relatively unchanged over k except for the stable regions at the edges in Fig. 2. The weighting factor for ϵ_y is much larger (~ 40) than that for ϵ_z (~ 3). Therefore, in order to have equivalent effect, only a fraction of the momentum spread ($\epsilon_y \leq 0.1 \epsilon_z$) is sufficient for the energy spread.

Examination of the dispersion equation (4) yields that there exists an upper limit of the growth rate, given by $|\tilde{\Delta}_1| \leq \min \{3^{1/2}/2, \pi/4\tilde{\epsilon}_1\tilde{\epsilon}_2\}$. The absolute maximum growth rate $\tilde{\Delta}_1 = 3^{1/2}/2$ occurs for the zero temperature ($\tilde{\epsilon}_1 = \tilde{\epsilon}_2 = 0$) electron beam at the beam-waveguide synchronous ($\Omega_s = \omega_{ln}$) mode ($\tilde{a} = 0$). This shows that the rate of energy extraction from beam electrons is highest when the beam and the waveguide modes are synchronous. The possible maximum gain reduces as the spread ($\tilde{\epsilon}_1$ or $\tilde{\epsilon}_2$) increases. Equation (4) also shows that the instability region is bounded in a \tilde{a} -space by $\tilde{a}_+ > \tilde{a} > \tilde{a}_-$. The instability boundaries \tilde{a}_+ and \tilde{a}_- are given in Fig. 3. The lower bound \tilde{a}_- is a decreasing function of $\tilde{\epsilon}_2$ (or $\tilde{\epsilon}_1$), while the upper bound \tilde{a}_+ is a decreasing function of $|\tilde{\epsilon}_1 - \tilde{\epsilon}_2|$ with its maximum at $\tilde{\epsilon}_1 = \tilde{\epsilon}_2$. Since the upper limit of \tilde{a} is experimentally imposed by wall radius R (see Fig. 2) unless the spreads are very large, in which case it is determined by \tilde{a}_+ it is found that for small $\tilde{\epsilon}$ the unstable range in k is determined by \tilde{a}_- . Therefore we conclude that the unstable bandwidth in the wave number k becomes broader as the spreads increase.

Finally we proceed to find the eigenvalue $\tilde{\lambda}$ by numerically solving eq. (4) for given \tilde{a} , $\tilde{\epsilon}_1$ and $\tilde{\epsilon}_2$. The results are shown in Fig. 4. The growth rates contours are drawn in $\tilde{\epsilon}_1$ - $\tilde{\epsilon}_2$ space for four representative values of \tilde{a} (1,0,-1,-2). The instability region in spread space becomes broader as \tilde{a} decreases due to \tilde{a}_+ curve (see Fig. 3), but as \tilde{a} further decreases (e.g., $\tilde{a} = -2$), a new stable region appears near $\tilde{\epsilon}_1 = \tilde{\epsilon}_2 = 0$ due to \tilde{a}_- curve. The maximum growth rate in spread space occurs at $\tilde{\epsilon}_1 = \tilde{\epsilon}_2 = 0$ in general, but as \tilde{a} decreases, the point, marked by a filled square, moves along $\tilde{\epsilon}_1 = 0$ (or $\tilde{\epsilon}_2 = 0$) line (e.g., $\tilde{a} = -2$). This phenomenon is readily explained when we note that at out of synchronization mode ($\tilde{a} \neq 0$) the spreads provide a fraction of electrons that are synchronous, while at the synchronous mode ($\tilde{a} = 0$) the spreads reduce the number of synchronous electrons. Gyrotron amplifiers are usually operated near $\tilde{a} = 0$. With parameters given in Fig. 2, the minimum spreads needed to stabilize the instability are found to be 3.4% and 49.2% for the energy and the momentum at the synchronous case. Near the beam-waveguide synchronous mode (i.e., $\Omega_s \sim \omega_{ln}$) the instability is stabilized with the spreads for low $\tilde{\epsilon}$, while the growth rate is maximum at $\tilde{\epsilon}_1 = \tilde{\epsilon}_2$ for high $\tilde{\epsilon}$. The reverse is true for an out-of synchronization mode (i.e., $|\Omega_s - \omega_{ln}| \gg 0$). The opposite behavior of the growth rate on the spreads at high $\tilde{\epsilon}$ may be significant if the spreads increase during the interaction stage.

We note that at the synchronous mode the growth rate becomes highest along the $\tilde{\epsilon}_1 = \tilde{\epsilon}_2$ line in Figs. 4 (the case $\tilde{a} = 0$). At the synchronous condition where the conducting wall radius R is adjusted to have the beam mode Ω_s curve graze the waveguide ω_{ln} curve, the line $\tilde{\epsilon}_1 = \tilde{\epsilon}_2$ corresponds that $\beta_{\perp}^2 \epsilon_{\perp} = 2\beta_z^2 \epsilon_z$, where ϵ_{\perp} refers to the spread in the transverse momentum. This means that

the thermal temperature of the beam electrons is isotropic. In other words, at the synchronous wave number the amplifier becomes most efficient when the beam distribution is isotropic.

It is worthwhile to emphasize that the reduced dispersion equation (4) coupled with the normalization equation (3) describes the entire spectrum of mode s , l , n , and k . Once the mode is identified, eq. (3) determines the numerical values of \tilde{a} , $\tilde{\epsilon}_1$ and $\tilde{\epsilon}_2$ to find the growth rate $\tilde{\lambda}_i$ via eq. (4), which in turn is transformed to the actual Δ_i through eq. (3). Therefore, the mode spectral analysis is reduced to determination of the scaling factor eq. (3).

The authors would like to acknowledge the benefit of the useful discussions with H. Uhm.

References

1. R. Q. Twiss, *Aus. J. Phys.* 11, 564 (1958).
2. J. Schneider, *Phys. Rev. Letts.* 2, 504 (1959).
3. A. V. Gaponov, *Izv. VUZ. Radiofizika* 2, 450 (1959)
and Addendum, *ibid*, p. 837 (1959).
4. P. Sprangle and A. T. Drobot, *IEEE Trans. MTT-25*, 528 (1977);
K. R. Chu, *NRL Memo Rep.* 3672 (1977); M. Read and R. Lucey,
JAYCOR Rep. 2061, *NRL Contract No.* N00173-77-C-0215 (1978).
5. A. V. Gaponov, M. I. Petelin and V. K. Yulpatov, *Radio Phys. Quant.*
Elect. 10, 9, 794 (1967).
6. J. L. Hirshfield and V. L. Granatstein, *IEEE Trans. MTT-25*, 522 (1977);
See also V. A. Flyagin, A. V. Gaponov, M. I. Petelin and V. K. Yulpatov,
ibid, No. 6, p. 514 (1977)
7. K. R. Chu, *Phys. Fluids* 21, 2354 (1978).
8. H. Uhm, R. C. Davidson and K. R. Chu, *Phys. Fluids* 21, 1866 (1978).
9. J. Y. Choe and S. Ahn, *NRL Memo Rep.* 4041 (1979).
10. V. L. Granatstein, L. Seftor, L. Barnett, M. Read, K. R. Chu and
P. Sprangle, *IEEE Int'l. Conf. on Plasma Sci.*, June 4-6 (1979).
11. H. R. Jory, S. J. Evans, S. J. Hegji, J. F. Shively, R. S. Symons and
N. J. Taylor, *IEEE Int'l. Conf. on Plasma Sci.*, June 4-6 (1979).
12. We note that the growth rate is dominantly governed by the beam resonance
term (Δ in eq. (1)), and as can be seen in the expression for Δ ($\equiv \omega - \Omega_s$), it is
independent of P_θ . Therefore, the effect of the spread in the canonical angular
momentum is much smaller than those in the energy or axial momentum.
13. J. Y. Choe and S. Ahn, *NRL Memo Rep.* 4035 (1979).

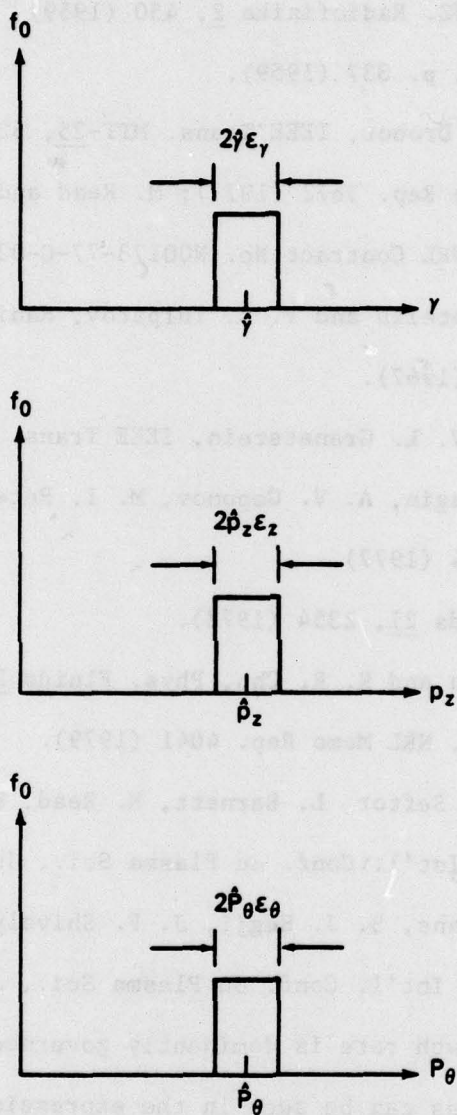


Fig. 1 - Equilibrium distribution function of beam electrons

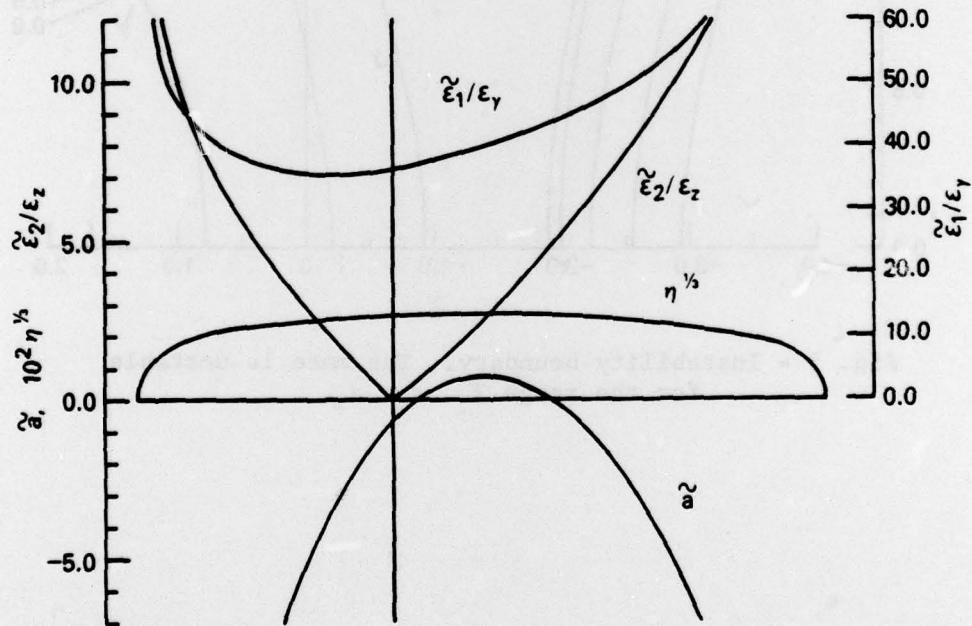
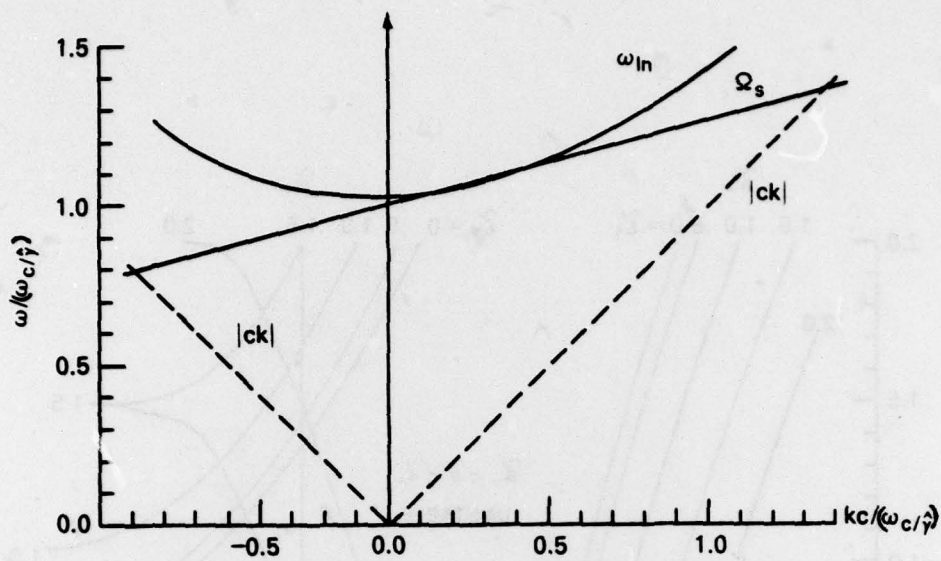


Fig. 2 - Doppler shifted beam mode (Ω_s) and the waveguide mode (ω_{ln}) vs. the axial wavenumber k , and the corresponding normalization factor $(nb)^{1/3}$, $\tilde{\epsilon}_1/\epsilon_\gamma$, $\tilde{\epsilon}_2/\epsilon_z$ and the normalized \tilde{a} vs. k . For actual parameters see text.

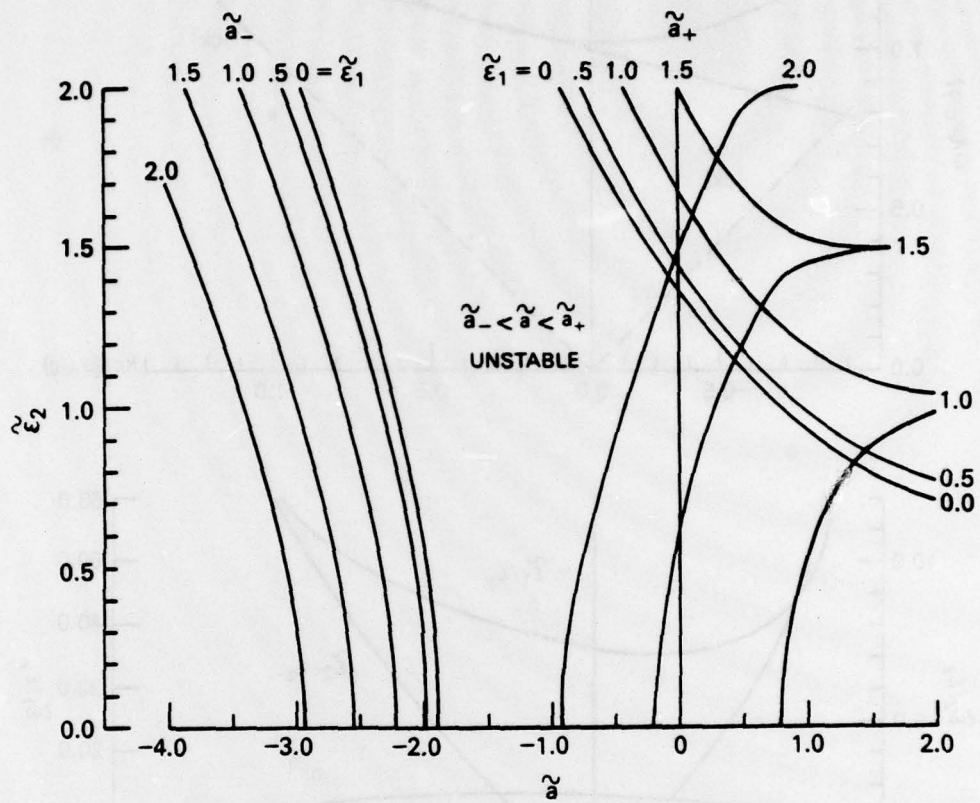


Fig. 3 - Instability boundary. The mode is unstable for the range $\tilde{a}_- < \tilde{a} < \tilde{a}_+$.

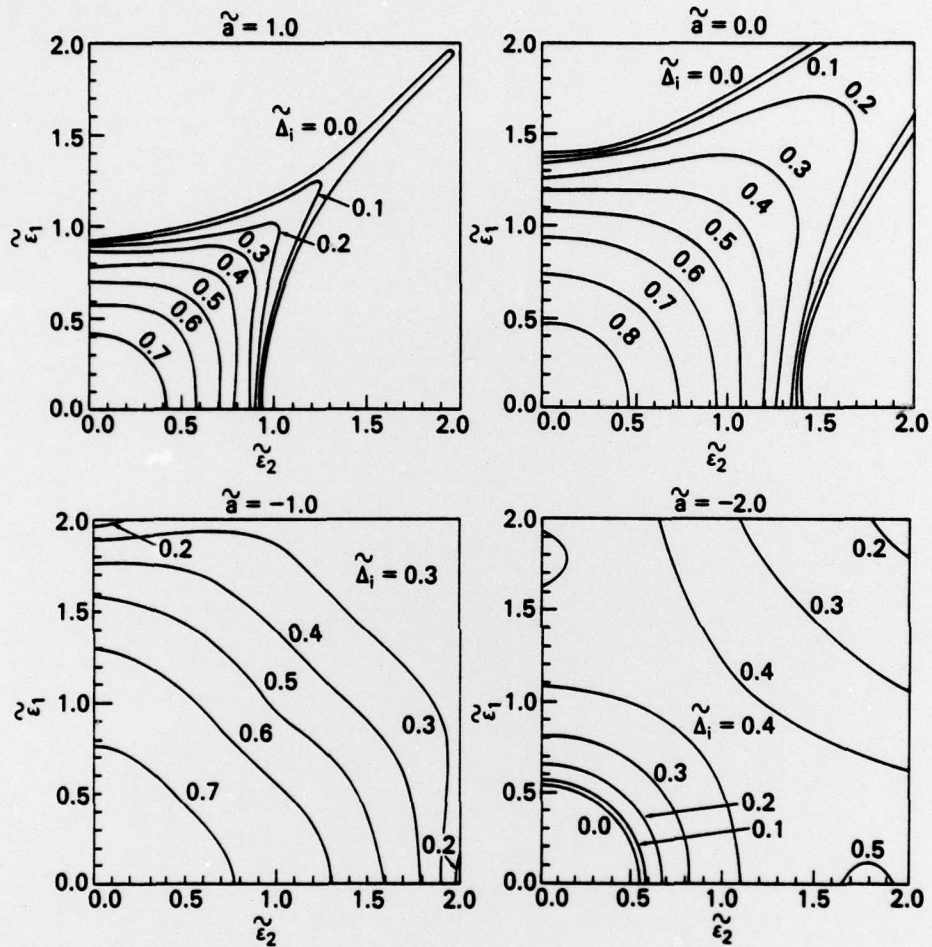


Fig. 4 - Growth rate contours for $\tilde{a} = 1, 0, -1, -2$

Accession For	
NTIS GRI&I	<input checked="" type="checkbox"/>
DDC TAB	<input type="checkbox"/>
Unannounced	<input type="checkbox"/>
Justification _____	
By _____	
Distribution/ _____	
Availability Codes	
Dist	Avail and/or special
A	